

Magnetic state of Ce in thin layers

Y. Aoki,* H. Sato, Y. Komaba, Y. Kobayashi, H. Sugawara, S. Hashimoto, T. Yokoyama, and T. Hanyu
Department of Physics, Faculty of Science, Tokyo Metropolitan University, Hachioji-shi, Tokyo 192-03, Japan
 (Received 29 March 1996; revised manuscript received 25 June 1996)

We have fabricated Ce/Ta multilayers under ultrahigh vacuum to investigate the magnetic state of Ce in thin layers. The magnetization, electrical resistivity, and Hall effect have been measured for Ce layer thicknesses between 5 and 100 Å. Results of x-ray analysis indicate that Ce atoms crystallize as bulk Ce for $d_{\text{Ce}}=100$ Å, and are amorphous for $d_{\text{Ce}}\leq 15$ Å. For $d_{\text{Ce}}=100$ Å, the Ce γ - α transition observed in the resistivity and reduced magnetization at 2 K suggest the stabilization of α -phase Ce at low temperatures. For $d_{\text{Ce}}\leq 15$ Å, in contrast, the magnetic susceptibility and extraordinary Hall effect indicate the existence of magnetic Ce down to 1 K. We speculate that the transition to the nonmagnetic state of Ce at low temperatures for $d_{\text{Ce}}\leq 15$ Å is prevented by the amorphous structure. [S0163-1829(96)02341-7]

I. INTRODUCTION

The anomalous magnetic behavior of Ce metal has been intensively studied for many years.^{1,2} Ce metal is known to have three different crystallographic structures at ambient pressure, i.e., fcc α , dhcp β , and fcc γ . At low temperatures, the α phase is stable, and behaves as an enhanced Pauli paramagnet with quenched $4f$ magnetic moments. With increasing temperature, the α phase transforms to the β phase, and then to the γ phase. The β phase disappears at pressures greater than 2 kbar. The β and γ phases are characterized by localized $4f$ magnetic moments with Curie-Weiss behavior of the magnetic susceptibility. The mechanisms of the γ - α and β - α phase transitions in Ce have been intensively studied.¹ However, experimental investigations have been limited to bulk systems including pressure effect and substitution effect with Th and La.^{3,4}

As a different approach to investigation of the Ce magnetic state, we have focused on Ce/Ta multilayers. Recently, preparation techniques for artificial multilayers have been improved. Using ferromagnetic/nonmagnetic and superconducting/normal-metal multilayers, areas including the giant magnetoresistance effect, confirmation of Ruderman-Kittel-Kasuya-Yosida interaction, and the dimensionality of superconductivity have been investigated. However, studies on the unstable $4f$ state in multilayers have not been carried out.

As a nonmagnetic intervening layer, we selected bcc Ta. Since Ta is immiscible with Ce, the system has the advantages of no alloying and no intermetallic compound formation in the interfacial region. In this work, we present the results of magnetization M , resistivity ρ , and Hall resistivity ρ_{xy} measurements for Ce/Ta multilayers with various Ce layer thicknesses, d_{Ce} .

II. EXPERIMENTAL DETAILS

The Ce/Ta multilayers were deposited from E -gun sources onto Si(111) substrates at room temperature to reduce the possibility of island formation, which degrades the quality of layered structures. The background pressure in the evaporating system was lower than 1×10^{-10} Torr. The

ultrahigh-vacuum condition is essential to reduce the oxidation of Ce layers. First, we deposited a 50-Å-thick Ta buffer layer to prevent reaction of Ce with the Si substrate. Then we fabricated Ce/Ta multilayers of the form $[\text{Ce}(d_{\text{Ce}} \text{ Å})/\text{Ta}(d_{\text{Ta}} \text{ Å})]_N$, where the Ce layer thickness d_{Ce} was varied from 5 to 100 Å, while the Ta layer thickness d_{Ta} was constant at 15 Å. $N=100$ for $d_{\text{Ce}}=5$ Å and $N=10$ for $d_{\text{Ce}}=100$ Å. Finally, we deposited a 50-Å-thick Ta cover layer to reduce oxidation of the Ce layers. The thickness of each layer was controlled using a film thickness monitor. The samples were examined by x-ray diffraction (Cu K_α).

The magnetization measurements were performed using a commercial superconducting quantum interference device magnetometer. The applied magnetic field was parallel to the sample plane. Subtraction of the Si substrate contribution, which is comparable to that of the Ce/Ta multilayers, results in errors of a few percent. The electrical resistivity and Hall resistivity measurements were performed by a standard four-probe dc method using Keithley 182 nanovoltmeters. The contribution of the Si substrate ($\sim 10^2 \Omega \text{ cm}$ at room temperature) to the electrical resistivity and Hall resistivity is negligible.

III. RESULTS AND DISCUSSION

In Fig. 1, we show the low-angle x-ray-diffraction spectra in which several peaks are observed corresponding to the multilayer periodicity λ . The estimated values of λ are 50 ± 6 Å for Ce(30 Å)/Ta(15 Å), 36 ± 4 Å for Ce(15 Å)/Ta(15 Å), and 25 ± 2 Å for Ce(8 Å)/Ta(15 Å), which agree with the designed values to within $\sim 10\%$. Figure 2 shows the high-angle x-ray-diffraction spectra. For $d_{\text{Ce}}=100$ Å, peaks corresponding to bulk γ -Ce are observed, suggesting that Ce crystallizes in the same form as bulk Ce; clear peaks corresponding to bulk β -Ce were not observed. For $d_{\text{Ce}}=15$ and 5 Å, no obvious peaks corresponding to crystallized Ce are identified. This indicates that the Ce layers in these samples do not crystallize but are rather amorphous. This is expected, since d_{Ce} values of 15 and 5 Å correspond to only a few atomic layers of Ce.

The field dependence of magnetization $M(H)$ at 2 K is shown in Fig. 3. No spontaneous magnetization is observed.

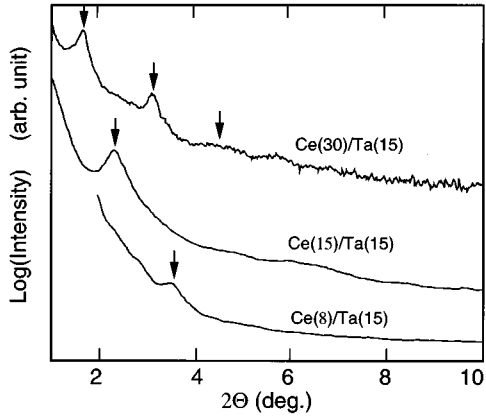


FIG. 1. Low-angle x-ray-diffraction spectra ($\text{Cu } K_\alpha$) for $d_{\text{Ce}} \leq 30$ Å.

For $d_{\text{Ce}} = 15$ and 5 Å, M increases with increasing magnetic field obeying a Brillouin function. The extrapolated saturation magnetization ($\sim 1 \mu_B/\text{Ce}$) is similar to the values usually observed for Ce compounds containing Ce^{3+} . In contrast, M for $d_{\text{Ce}} = 100$ Å is reduced to $0.2 \mu_B/\text{Ce}$ at 5.5 T, although this value is still larger than that of $0.005 \mu_B/\text{Ce}$ at 5.5 T expected for α -Ce (Ref. 5).

Figure 4 shows the temperature dependence of M below 50 K measured at 5 T. No indication of magnetic transition is observed. The temperature dependence of $1/M$ obeys the Curie-Weiss law, indicating that the Ce ions are in the paramagnetic state. The reduced magnetization for $d_{\text{Ce}} = 100$ Å, which is evident at low temperatures, seems to be associated with an enhanced negative Weiss temperature of $\Theta_p \sim -20$ K.

Figure 5 shows the temperature dependence of the resistivity $\rho(T)$ for $d_{\text{Ce}} = 100$ Å with the data for bulk Ce (Ref. 6). The resistivity for $d_{\text{Ce}} = 100$ Å decreases with decreasing temperature in approximately the same way as that for bulk Ce, except that there is a large residual resistivity. ρ shows a sudden drop at around 60 K with decreasing temperature and, with increasing temperature, ρ gradually increases without such an anomaly up to 200 K, at which the thermal

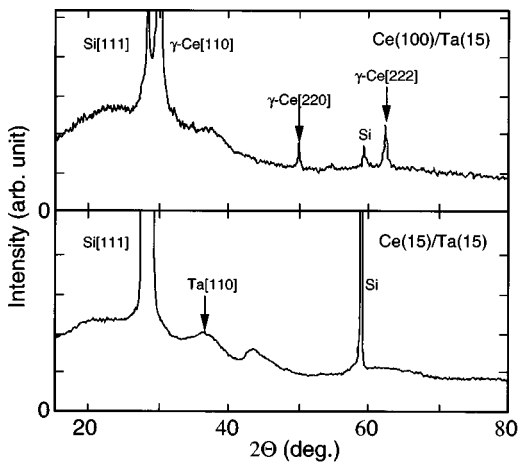


FIG. 2. High-angle x-ray-diffraction spectra ($\text{Cu } K_\alpha$) for $d_{\text{Ce}} = 15$ and 100 Å.

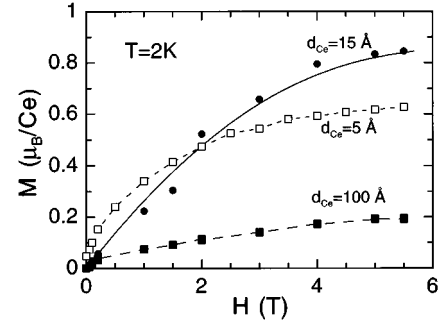


FIG. 3. Magnetization curves obtained at 2 K for $d_{\text{Ce}} = 5, 15,$ and 100 Å.

hysteresis loop is closed. This thermal hysteresis is similar to that of the γ - α transition in bulk Ce. The decrease in ρ near 10 K indicates the presence of precipitated β -Ce, which undergoes an antiferromagnetic transition at 12.5 K.

In contrast, the resistivity for $d_{\text{Ce}} = 15$ and 5 Å is larger and increases with decreasing temperature as shown in Fig. 6. This is due to disorder scattering in the Ce amorphous layers. The larger resistivity for $d_{\text{Ce}} = 15$ Å compared with that for $d_{\text{Ce}} = 5$ Å is consistent with this interpretation. As a simple prediction, the resistivity should be proportional to $d_{\text{Ce}}/(d_{\text{Ce}} + d_{\text{Ta}})$, and then $\rho(d_{\text{Ce}} = 5 \text{ Å})/\rho(d_{\text{Ce}} = 15 \text{ Å})$ would be $1/2$. Taking into account that $\rho(d_{\text{Ce}} = 5 \text{ Å})/\rho(d_{\text{Ce}} = 15 \text{ Å}) < 1/2$, however, it is possible that the adjacent Ta layers are shortened through the intervening Ce layer for $d_{\text{Ce}} = 5$ Å. $\ln T$ dependence of ρ is seen below 20 K for $d_{\text{Ce}} = 5$ Å and below 50 K for $d_{\text{Ce}} = 15$ Å. Such behavior has two possible origins; weak localization^{7,8} (WL) and the Kondo effect. If the $\ln T$ dependence was due to the Kondo effect, the Kondo temperature T_K would be higher than 10 K. This is not consistent with the low Weiss temperature Θ_p of 3 – 5 K. Therefore, we infer that the $\ln T$ dependence of $\rho(T)$ is mainly due to the WL effect.

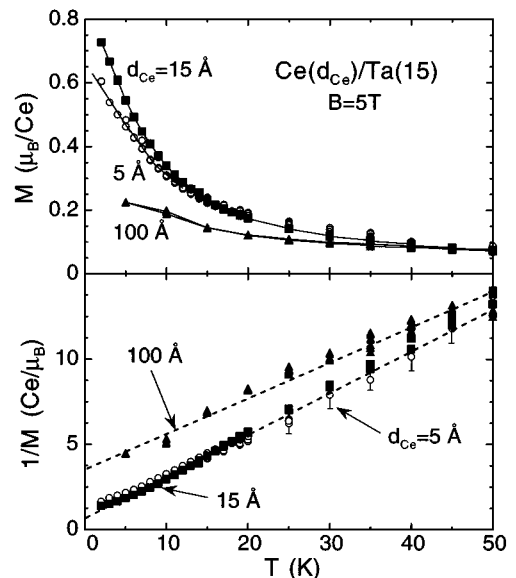


FIG. 4. Temperature dependence of magnetization M and $1/M$ for $d_{\text{Ce}} = 5, 15,$ and 100 Å obtained at a field of 5 T applied parallel to the sample plane.

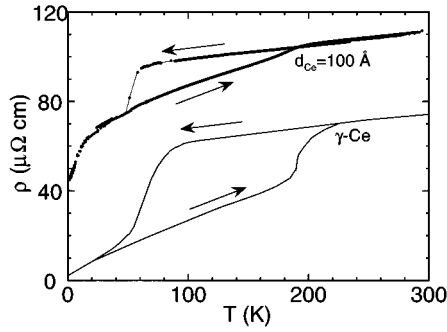


FIG. 5. Temperature dependence of resistivity $\rho(T)$ for $d_{\text{Ce}}=100 \text{ \AA}$. The data reported by Burgardt *et al.* (Ref. 6) for bulk Ce is also shown.

The temperature dependence of the Hall resistivity ρ_{xy} , measured at $H=1 \text{ T}$ is shown in Fig. 7. At room temperature, the Hall coefficient R_H , which is defined as ρ_{xy}/H , is $+2 \times 10^{-10} \text{ m}^3/\text{C}$ for $d_{\text{Ce}}=15 \text{ \AA}$ and $+0.9 \times 10^{-10} \text{ m}^3/\text{C}$ for $d_{\text{Ce}}=100 \text{ \AA}$. These values are similar to the reported values of $+2.0 \times 10^{-10} \text{ m}^3/\text{C}$ for $\gamma\text{-Ce}$ (Ref. 9) and $+1.0 \times 10^{-10} \text{ m}^3/\text{C}$ for polycrystalline Ta film (Ref. 10) at room temperature. Below 50 K, there appears to be a large difference in $\rho_{xy}(T)$ for $d_{\text{Ce}}=15$ and 100 \AA ; $\rho_{xy}(T)$ increases largely for $d_{\text{Ce}}=15 \text{ \AA}$ with decreasing temperature, while it levels off for $d_{\text{Ce}}=100 \text{ \AA}$. ρ_{xy} is usually expressed as

$$\rho_{xy} = R_0 H + R_S M, \quad (1)$$

where R_0 is the normal Hall coefficient and R_S is the extraordinary Hall coefficient representing the magnitude of asymmetric magnetic scattering of conduction electrons. Since the temperature dependence of ρ_{xy} is similar to that of M in Fig. 4, the temperature dependence of ρ_{xy} can be attributed to the extraordinary Hall effect. In fact, ρ_{xy} plotted against M is approximately linear for $d_{\text{Ce}}=15 \text{ \AA}$ (not shown), and R_0 and R_S are determined as $+1 \times 10^{-10} \text{ m}^3/\text{C}$ and $+6.1 \times 10^{-8} \text{ m}^3/\text{C}$, respectively. The temperature independence of R_S is reasonable since R_S generally depends on the electrical resistivity¹¹ and the resistivity is approximately temperature independent for $d_{\text{Ce}}=15 \text{ \AA}$. The field dependence of Hall resistivity $\rho_{xy}(H)$ at 1.5 and 4.2 K is shown in Fig. 8. ρ_{xy} for $d_{\text{Ce}}=15 \text{ \AA}$ is larger than that for $d_{\text{Ce}}=100 \text{ \AA}$, and has down-

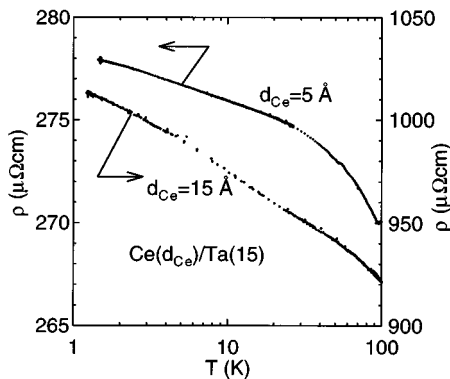


FIG. 6. Logarithmic temperature dependence of resistivity $\rho(T)$ for $d_{\text{Ce}}=5$ and 15 \AA .

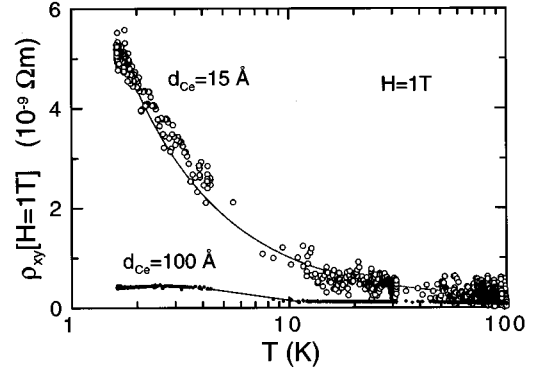


FIG. 7. Temperature dependence of Hall resistivity ρ_{xy} measured at $H=1 \text{ T}$, for $d_{\text{Ce}}=15$ and 100 \AA .

ward curvature in a similar way to the $M(H)$ curves in Fig. 3. This also indicates that ρ_{xy} is mainly due to the extraordinary Hall effect. These results for the Hall effect confirm the above-mentioned interpretation.

In the present investigation, we demonstrate that Ce for $d_{\text{Ce}}=100 \text{ \AA}$ crystallizes as bulk Ce and has reduced magnetic moments indicating the presence of $\alpha\text{-Ce}$ at low temperatures. For $d_{\text{Ce}}=15 \text{ \AA}$, in contrast, the amorphous Ce phase is stabilized and a stable magnetic moment similar to that of $\gamma\text{-Ce}$ is maintained down to 1 K. It is concluded that the 4f state for $d_{\text{Ce}}=15 \text{ \AA}$ is an extraordinary state and different from that of usual metallic Ce. The transition to nonmagnetic Ce at low temperatures might be prevented by the amorphous structure.

In the pressure-temperature phase diagram for Ce metal, the $\gamma\text{-}\alpha$ phase-transition temperature decreases with decreas-

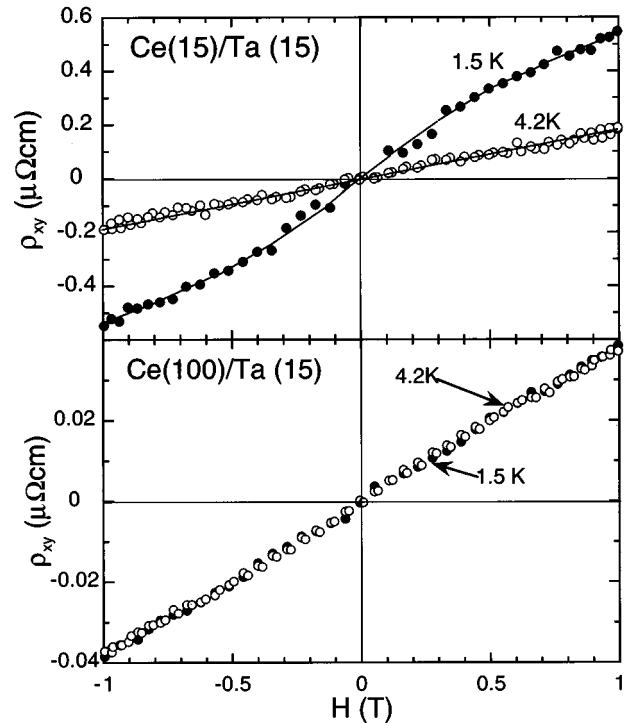


FIG. 8. Field dependence of Hall resistivity ρ_{xy} for $d_{\text{Ce}}=15$ and 100 \AA .

ing pressure.^{1,2} Therefore, if Ce forms small crystal grains and there is a negative chemical pressure in the Ce/Ta multilayers for $d_{\text{Ce}}=5$ and 15 Å, the γ - α phase transition will occur at lower temperatures. However, this mechanism is not plausible in the present experiment, since large-scale epitaxial growth is not possible because Ce is immiscible with Ta. Even if epitaxial growth occurred locally, the chemical pressure would be positive since the in-plane atomic density is 0.13 atoms/Å² for the [110] plane of bcc-Ta and 0.09 atoms/Å² for the [111] plane of fcc-Ce. For $d_{\text{Ce}}=100$ Å, the γ - α transition temperature determined from the results for $\rho(T)$ is similar to that for bulk Ce metal, suggesting that there is no appreciable chemical pressure, at least for $d_{\text{Ce}}=100$ Å.

For the γ - α phase transition in Ce metal, three main theoretical explanations have been proposed. (1) In the promotion model (valence change model),^{12,13} it is assumed that the γ - α transition is due to the promotion of f electrons in the γ phase into the conduction band in the α phase which has a lower volume. This model is difficult to reconcile with photoemission data.¹⁴ (2) In the Mott transition (MT) model,¹⁵ the γ - α transition is assumed to be a transition from a state with localized f electrons to a state with delocalized f electrons forming Bloch states. (3) In the Kondo volume collapse (KVC) model,^{16,17} the γ - α transition is assumed to be governed by spin screening of the localized f electrons by the conduction electrons. In this model the γ phase has unscreened localized moments, while the α phase has screened moments. Thus, in both the MT model and the KVC model, the γ phase of Ce contains localized f electrons, while the nature of the α phase is a subject of discussion.

Based on the MT model, it is speculated that the amorphous structure for $d_{\text{Ce}}\leq 15$ Å prevents the formation of the f band which results in nonmagnetic Ce. In fact, Eriksson *et al.*¹⁸ predicted, based on their calculations, that the surface of bulk α -Ce, where atomic translational symmetry is broken, should behave like magnetic γ -Ce. In the KVC model, it

is assumed that the system is composed of independent non-interacting Kondo sites, and the Kondo lattice effect is neglected. That is, the model does not depend on whether the sample is crystalline or amorphous. Considering the clear difference in the magnetic properties of the crystalline and amorphous Ce in the present experiment, we should take into account the Kondo lattice effect if we use the KVC model.

As another possible origin of the different magnetic behaviors for $d_{\text{Ce}}=100$ Å and $d_{\text{Ce}}\leq 15$ Å, we cannot rule out the possibility of a three-dimensional to two-dimensional transition of the Ce ion electronic state. However, it is difficult to use the present results to discuss the dimensionality, since the arrangement of Ce ions in the present samples is not ideal. Epitaxial growth in our samples is not expected due to the lattice mismatch between Ce and Ta, which leads to the immiscibility of the two elements.

In summary, we have measured the magnetization M , resistivity ρ , and Hall resistivity ρ_{xy} of Ce/Ta multilayers with various Ce layer thicknesses, d_{Ce} . X-ray analysis indicates the existence of crystalline Ce for $d_{\text{Ce}}=100$ Å and amorphous Ce for $d_{\text{Ce}}\leq 15$ Å. For $d_{\text{Ce}}=100$ Å, the resistivity shows an anomaly reflecting the γ - α transition and the magnetization is reduced at 2 K, which indicates the presence of stabilized α -phase Ce at low temperatures. For $d_{\text{Ce}}\leq 15$ Å, in contrast, the magnetic susceptibility and extraordinary Hall effect indicate that the magnetic moments of Ce are stable at low temperatures. Thus we conclude that the effect of the local environment of Ce is important in the magnetic-nonmagnetic phase transition of Ce at low temperatures.

ACKNOWLEDGMENTS

We would like to thank T. Nishigaki for technical support and Professor Kunihiko Maezawa for helpful discussions. This work was partly supported by a Grant-in-Aid for Scientific Research from the Ministry of Education, Science and Culture.

*Correspondence to Dr. Yuji Aoki, Department of Physics, Faculty of Science, Tokyo Metropolitan University, Hachioji, Tokyo 192-03, Japan. FAX: +81-426-77-2483; Electronic address: aoki@phys.metro-u.ac.jp.

¹D. C. Koskenmaki and K. A. Gschneidner, Jr., in *Handbook on the Physics and Chemistry of Rare Earths*, Vol. 1, edited by K. A. Gschneidner and L. Eyring (North-Holland, Amsterdam, 1978), Chap. 4.

²J. M. Lawrence, P. S. Riseborough, and R. D. Parks, *Rep. Prog. Phys.* **44**, 1 (1981).

³G. Oomi, *J. Phys. Soc. Jpn.* **48**, 857 (1980).

⁴J. D. Thompson, Z. Fisk, J. M. Lawrence, J. L. Smith, and R. M. Martin, *Phys. Rev. Lett.* **50**, 1081 (1983).

⁵D. C. Koskenmaki and K. A. Gschneidner, Jr., *Phys. Rev. B* **11**, 4463 (1975).

⁶P. Burgardt, K. A. Gschneidner, Jr., D. C. Koskenmaki, D. K. Finnemore, J. O. Moorman, S. Legvold, C. Stassis, and T. A. Vyrostek, *Phys. Rev. B* **14**, 2995 (1976).

⁷S. Hikami, A. I. Larkin, and Y. Nagaoka, *Prog. Theor. Phys.* **63**, 707 (1980).

⁸G. Bergmann, *Phys. Rep.* **107**, 1 (1984).

⁹C. J. Kevane, S. Legvold, and F. H. Spedding, *Phys. Rev.* **91**, 1372 (1953).

¹⁰A. W. Smith, *Phys. Rev.* **8**, 79 (1916).

¹¹L. Berger and G. Bergmann, in *The Hall Effect and its Applications*, edited by C. L. Chien and C. R. Westgate (Plenum, New York, 1979), p. 55.

¹²B. Coqblin and A. Blandin, *Adv. Phys.* **17**, 281 (1968).

¹³R. Ramirez and L. M. Falicov, *Phys. Rev. B* **3**, 1225 (1971).

¹⁴E. Willoud, H. R. Moser, W. -D. Schneider, and Y. Baer, *Phys. Rev. B* **28**, 7354 (1983).

¹⁵B. Johansson, *Philos. Mag.* **30**, 469 (1974).

¹⁶J. W. Allen and R. M. Martin, *Phys. Rev. Lett.* **49**, 1106 (1982).

¹⁷M. Lavagna, C. Lacroix, and M. Cyrot, *J. Phys. F* **13**, 1007 (1983).

¹⁸O. Eriksson, R. C. Albers, A. M. Boring, G. W. Fernando, Y. G. Hao, and B. R. Cooper, *Phys. Rev. B* **43**, 3137 (1991).